Published online 7 June 2021

Nucleic Acids Research, 2021, Vol. 49, No. 11 ***6331–6346***
https://doi.org/10.1093/nar/gkab458

LEO1 is a partner for Cockayne syndrome protein B (CSB) in response to transcription-blocking DNA damage

Vinod Tiwari [1], Tomasz Kulikowicz[1], David M. Wilson, 3rd[2,*] and Vilhelm A. Bohr [1,*]

[1]Section on DNA repair, National Institute on Aging, National Institutes of Health, Baltimore, MD 21224, USA and [2]Hasselt University, Biomedical Research Institute, 3590 Diepenbeek, Belgium

Received March 05, 2021; Revised May 04, 2021; Editorial Decision May 10, 2021; Accepted June 03, 2021

ABSTRACT

Cockayne syndrome (CS) is an autosomal recessive genetic disorder characterized by photosensitivity, developmental defects, neurological abnormalities, and premature aging. Mutations in CSA (ERCC8), CSB (ERCC6), XPB, XPD, XPG, XPF (ERCC4) and ERCC1 can give rise to clinical phenotypes resembling classic CS. Using a yeast two-hybrid (Y2H) screening approach, we identified LEO1 (Phe381-Ser568 region) as an interacting protein partner of full-length and C-terminal (Pro1010-Cys1493) CSB in two independent screens. LEO1 is a member of the RNA polymerase associated factor 1 complex (PAF1C) with roles in transcription elongation and chromatin modification. Supportive of the Y2H results, purified, recombinant LEO1 and CSB directly interact *in vitro*, and the two proteins exist in a common complex within human cells. In addition, fluorescently tagged LEO1 and CSB are both recruited to localized DNA damage sites in human cells. Cell fractionation experiments revealed a transcription-dependent, coordinated association of LEO1 and CSB to chromatin following either UVC irradiation or cisplatin treatment of HEK293T cells, whereas the response to menadione was distinct, suggesting that this collaboration occurs mainly in the context of bulky transcription-blocking lesions. Consistent with a coordinated interaction in DNA repair, LEO1 knockdown or knockout resulted in reduced CSB recruitment to chromatin, increased sensitivity to UVC light and cisplatin damage, and reduced RNA synthesis recovery and slower excision of cyclobutane pyrimidine dimers following UVC irradiation; the absence of CSB resulted in diminished LEO1 recruitment. Our data indicate a reciprocal communication between CSB and LEO1 in the context of transcription-associated DNA repair and RNA transcription recovery.

INTRODUCTION

CS is a rare and fatal autosomal recessive segmental progeria characterized by failure to thrive early in life, impaired development, and unique physical traits (e.g., 'birdlike' facies), sensorineural deafness, progressive visual loss, and neurological degeneration, along with increased sensitivity to ultraviolet (UV) light (1,2). Genetic defects in the *ERCC8* (CSA) or *ERCC6* (CSB) genes, which give rise to classic CS (3), result in the inability to recover RNA synthesis following UV irradiation, suggesting a function for the proteins in resolving transcription-blocking DNA lesions. CSB is a DNA-dependent ATPase from the SWI2/SNF2 family, which includes proteins that operate as chromatin remodelers (4). CSA has no known enzymatic function but harbors several WD40 repeat motifs that facilitate specific protein interactions, such as within the DDB1–CUL4–RBX1 (CRL4) ubiquitin ligase complex (5). Collectively, important biological roles for the CSA and CSB proteins have been reported in transcription-coupled nucleotide excision repair (TC-NER), transcriptional regulation (6), and mitochondrial function (7–11).

TC-NER is a component of NER that is specifically initiated upon stalling of RNA polymerase II (RNAPII) at a blocking lesion on the transcribed strand of an active gene (12). Bulky DNA damages like cyclobutane pyrimidine dimers (CPDs) and pyrimidine-(6,4)-pyrimidone photoproducts (6–4PPs), which are the predominant UV-induced DNA modifications, are examples of DNA lesions that impede RNAPII progression. A persistently stalled RNAPII signals recruitment of the TC-NER machinery, such as the key factor CSB, to the lesion site (3). Following RNAPII arrest, CSB interacts with stalled RNAPII, resulting in sequential recruitment of CSA, UVSSA and the transcription initiation factor IIH (TFIIH) complex (13). The CSB/CSA

*To whom correspondence should be addressed. Tel: +1 410 558 8162; Email: vbohr@nih.gov
Correspondence may also be addressed to David M. Wilson. Email: dmwilson3@outlook.com

complex interacts with stalled RNAPII and promotes ubiquitination of RNAPII (RPB1-K1268), facilitating subsequent recruitment of UVSSA to ubiquitinated RNAPII. UVSSA then orchestrates the transfer of TFIIH to stalled RNAPII (14,15). After initial DNA damage recognition, during either TC-NER or global genome NER (GG-NER), the helicase components of TFIIH (XPB and XPD) perform DNA opening and aid in lesion verification. XPA, along with TFIIH, RPA, XPF-ERCC1, XPG and PCNA, then perform strand incision on either side of the lesion to release a damage-containing DNA segment, followed by repair synthesis by POLδ, and nick ligation by either DNA LIG1 or XRCC1/LIG3α, depending on the cycling status of the cell (3).

The above findings indicate that the CS proteins function at the transcription-DNA repair interface. The transient CSB interaction with elongating RNAPII becomes more stable in the presence of transcription-stalling DNA lesions (16). Recent structural and functional analysis by cryo-electron microscopy from yeast showed that Rad26, the homologue of human CSB, alters the RNAPII path by binding DNA upstream of RNAPII and promoting the forward translocation of the polymerase (17). Moreover, Rad26 has been shown to displace Spt5 (transcription elongation factor and TC-NER repressor) from chromatin and promote error-free transcriptional bypass of DNA lesions (18). Hence, this translocating force of CSB facilitates RNAPII to bypass smaller obstructing lesions generated by oxidative DNA damage (19), whereas in the case of larger obstacles, it initiates TC-NER. Similarly, CSA is required for efficient repair during the elongation stages of RNAPII transcription (20).

In addition to its functions in facilitating repair and RNAPII activities, studies indicate that CSB is also involved in gene-specific transcriptional regulation. For example, CSB occupancy at promoters and enhancers increases in replicative cells (21,22), and similar observations have been reported for CSB under conditions of oxidative stress (23–25). Transcriptome analysis showed dysregulation of thousands of genes, including neuronal genes in CSB-deficient human fibroblasts (26). Moreover, Egly *et al.* demonstrated that CSB, the CSA–E3 ubiquitin ligase complex, and MDM2 are necessary for degradation of activating transcription factor 3 (ATF3), working collaboratively to restore transcription following DNA damage. Upon UV irradiation, ATF3 represses genes by binding to promoter sites, but by 12–24 h after UV irradiation, CS proteins help in ubiquitin-mediated proteasomal degradation of ATF3 to restore gene expression (27). However, in CS cells, chromatin bound ATF3 causes permanent transcriptional arrest and abrogates expression of its responsive genes (27,28). The tumor suppressor p53 is another interacting partner of both CS proteins, and CS cells exhibit an extended half-life of the p53 protein, apparently due to reduced polyubiquitination-mediated degradation (29–31). Collectively, these results indicate that CSB has direct and indirect roles in modulating transcriptional responses.

RNA polymerase-associated factor 1 complex (PAF1C) is an established elongation complex that consists of the PAF1, CDC73, LEO1, CTR9, RTF1 and SKI8 subunits in mammals. This complex has been demonstrated to play an important role in regulating transcription elongation, 3′ mRNA processing and chromatin remodeling (32). In addition, studies in yeast have reported a function of the complex members in facilitating Rad26-dependent TC-NER (33), as well as suppressing Rad26-independent TC-NER by cooperating with Spt4-Spt5 (34). We describe herein an interaction of CSB with LEO1, a component of PAF1C, and demonstrate a coordinated response of the two proteins to genotoxic damage, extending the molecular connection between the transcription machinery and the CS pathway.

MATERIALS AND METHODS

Yeast two-hybrid (Y2H) screen

The Y2H screen using C-terminal CSB (Pro1010-Cys1493) as bait was carried out by Dual Systems Biotech, Zurich, Switzerland (see Supplementary Figure S1).

Western blotting method

Standard western blot procedures were followed except for CSB detection. For CSB detection, after binding with anti-CSB antibody, the membrane was incubated with secondary horseradish peroxidase-conjugated antibody overnight and then processed using standard procedures. The following primary antibodies were used as per manufacturer's guidelines: anti-LEO1 (A300-175A; Bethyl Laboratories, Inc., TX, USA), anti-CSB antibodies (ab66598; Abcam, Cambridge, MA, USA), anti-PAF1, H3, and β-Actin (sc-514491, sc-517576 and sc-47778 respectively, Santa Cruz Inc., CA, USA). Secondary horseradish peroxidase-conjugated antibodies and ECL prime (GE Healthcare Bio-Sciences) or SuperSignal West Femto Chemiluminescent Substrates (Thermo Fisher Scientific) were used to visualize signals on a ChemiDoc XRS+ system (Bio-Rad Laboratories, Hercules, CA, USA). Digitized images were obtained, processed, and quantified with ImageLab version 6.1 (Bio-Rad Laboratories).

Protein interaction assay

Equal amount of recombinant LEO1 (100 ng) was incubated with or without human influenza hemagglutinin (HA) tagged-CSB (100 ng) in a 500 μl reaction containing 20 mM HEPES pH 7.9, 4 mM $MgCl_2$, 0.05 mM ATP, 40 g/ml bovine serum albumin (BSA) and 1 mM DTT at 4°C for overnight. CSB-bound protein was captured by incubating with anti-CSB antibody in the presence of A/G magnetic beads (88803, Thermo Fisher Scientific, Rockford, IL, USA) at 4°C for 1 h. The bead-protein interaction complex was washed three times with 20 mM HEPES pH 7.9, 4 mM $MgCl_2$, 1 mM DTT and 0.1% Nonidet *P*-40. The bead-bound protein complex was eluted by incubating with 4× lithium dodecyl sulfate (LDS) loading buffer at 95°C for 5 min and resolved on a 4–20% Bis–Tris-MOPS polyacrylamide gel (GenScript, Piscataway, NJ, USA) and detected by anti-CSB and anti-LEO1 antibodies via standard western blot techniques (see above). The recombinant wild-type CSB was purified as described previously (35) whereas LEO1 was obtained commercially (H00123169-P01; Novus

Biologicals, LLC, USA). The purity of recombinant proteins was visualized by using Silver Stain Plus Kit (Bio-Rad Laboratories, Hercules, CA, USA).

ATPase assay

ATPase assay was performed as described previously (35). Briefly, 10 μl ATPase reactions contained 20 mM HEPES–NaOH, pH 8.0, 1 mM $CaCl_2$, 0.05 mM ATP, 0.5 μCi of [γ-^{32}P] ATP, 40 μg/ml bovine serum albumin (BSA), 1 mM DTT and 150 ng of pUC19 plasmid DNA. Reactions were supplemented with 20 nM CSB alone and with increasing concentration of LEO1, as indicated. ATPase reactions were incubated for 1 h at 30°C and terminated by the addition of 5 μl of 0.5 M EDTA. 2 μl of each reaction mixture were spotted on polyethyleneimine thin-layer chromatography plates. Reaction products were separated using 1 M formic acid, 0.8 M LiCl mobile phase. The plates were exposed to a phosphorimager screen. The images were acquired on Typhoon FLA 9500 (Cytiva) and analyzed using ImageQuant TL software (GE Healthcare).

Co-immunoprecipitation method

Whole cell lysates (WCL) were prepared from untreated and UVC, cisplatin or menadione treated (as indicated) HEK293T cells or GFP-CSB expressing CS1AN cells by lysis in NP-40 lysis buffer (50 mM Tris pH 7.5, 150 mM NaCl, 1% Nonidet P40, 1 mM ethylenediaminetetraacetic acid (EDTA)) and complete protease inhibitor cocktail (Roche, Mannheim, Germany) for 20 min with rotation. Insoluble material was then removed by centrifugation at 14,000 rpm for 10 min at 4°C, and the supernatant was retained as WCL. To obtain the 'soluble chromatin fraction' (SC), insoluble material was dissolved in lysis buffer by sonication and benzonase A treatment for 20 min, and supernatant (SC) was harvested after centrifugation at 14,000 rpm for 10 min at 4°C. To prepare cytoplasmic extracts (CE), cells were incubated for 3 min on ice with CE buffer (10 mM HEPES, 60 mM KCl, 1 mM EDTA, 0.075% (v/v) NP-40, 1mM DTT and 1 mM PMSF, pH 7.6) and centrifuged at 1,500 rpm at 4°C to isolate supernatant (CE). The pellet was then dissolved in nuclear extract (NE) buffer (20 mM Tris–Cl, 420 mM NaCl, 1.5 mM $MgCl_2$, 0.2 mM EDTA, 1 mM PMSF and 25% (v/v) glycerol, pH 8.0), incubated on ice for 10 min, and centrifuged at 14,000 rpm for 10 min at 4°C to generate the NE.

Prior to immunoprecipitation, the WCL, NE and SC fractions were pretreated with protein A/G magnetic beads (Thermo Fisher Scientific) at 4°C for 1 h to remove non-specific protein binders. These extracts were then incubated as specified with either anti-LEO1 (A300-175A; Bethyl Laboratories, Inc., TX, USA) or anti-CSB antibodies (ab66598; Abcam, Cambridge, MA, USA) and with an isotype-matched IgG control for overnight. The immunocomplexes were subsequently captured by protein A/G magnetic beads for 1 h at 4°C. The bead-bound material was washed five times with wash buffer (10 mM Tris pH 7.5, 150 mM NaCl, 1% Triton-X-100, 1 mM EDTA and complete protease inhibitor cocktail), suspended in 4× LDS-PAGE loading dye, and incubated at 95°C for 5 min. Proteins were resolved on a polyacrylamide gel and detected by western blotting as described above.

Cell treatment conditions

Cells (HeLa, HeLa LEO1KD) were grown overnight to 70–80% confluency and then treated with the indicated chemical agent or 10 J/m^2 UVC. 200 μM cisplatin (479306–1G, Sigma, USA) treatment was given for 6 h or menadione (M5750-25G, Sigma, USA) treatment was given for 1 h at 200 μM concentration. Where indicated, cells were incubated with 100 μM 5,6-dichlorobenzimidazole 1-β-D-ribofuranoside (DRB) (D1916; Sigma, USA) for 1h and then treated with a genotoxin (i.e. UVC, cisplatin or menadione) at the designated dose and for the indicated time. Cisplatin and Menadione were added directly to the DRB containing medium. For the UVC experiment, after DRB treatment for 1 h, cells were irradiated with 10 J/m^2 UVC, and then allowed to recover for one hour prior to processing.

Cell line construction and maintenance

HEK293T and HeLa cells were grown in high glucose Dulbecco's modified Eagle's medium (DMEM) supplemented with 10% fetal calf serum and 1% penicillin/streptomycin. SV40-transformed CS1AN cells stably transfected with either CSB (CS1AN-CSB) or empty vector (CS1ANvector) and SH-SY5Y (see below) were cultured as above, except with 10% fetal bovine serum and 400 μg/ml geneticin (36). All cell lines were grown in a cell culture incubator maintained at 5% CO_2 and 37°C.

To knockdown LEO1 expression in HEK293T, HeLa, CS1AN and CS1AN-CSB cells, a plasmid vector containing one of the following shRNA sequences against LEO1 was used: 5′-CCGGGATTTAGGAAACGACTTATATC TCGAGATATAAGTCGTTTCCTAAATCTTTTTG-3′ (TRCN0000329746 Clone ID: NM_138792.2-1118s21c1) and 5′-CCGGCGCCGAGATGAAGAAGGAAATCT CGAGATTTCCTTCTTCATCTCGGCGTTTTTG-3′ (TRCN0000329745 Clone ID: NM_138792.2-1289s21c1, Santa Cruz Biotechnology, Dallas, TX, USA). A plasmid containing a scrambled shRNA was used as a control (Plasmid-A; Santa Cruz Biotechnology). Gene inactivation of LEO1 in SH-SY5Y cells was achieved by using the following guide RNAs in the $_p$LentiCRISPR v2 background: LEO1 CRISPR guide RNA 1 (AGGCTAATTCTGATGATGAA), RNA 2 (TGACTTACAACAGGCTGTCC) and RNA 3 (GAAGACAAACCACCTACTCC) (GenScript USA, Inc. piscataway, NJ). shRNA and CRISPR/Cas9 system components were delivered in cells using lentiviral vectors (psPAX2 and pCMV-VSVg plasmids; Addgene). Lentivirus generation and infections were performed as described previously (36). Briefly, 1μg of shRNA or guide RNA containing CRISPR plasmid was mixed with 750 ng of psPAX2 and 250 ng of pCMV-VSVg, and a master mix was created with lipofectamine 3000 in serum free media. After incubation for 30 min at room temperature, this master mix was added to HEK293T cells in antibiotic free media and incubated for 12–15 h. Media was replaced

with normal media after incubation and cells were further incubated in fresh media for 24 h. After 24 h incubation, media was harvested to collect lentiviral particles. For infection, HEK293T, HeLa, CS1AN, CS1AN-CSB and SH-SY5Y cells were incubated in normal culture media containing lentivirus and 8 μg/ml of polybrene overnight at 37°C. After 12–15 h, media was replaced with normal media and further incubated for 24 h. Subsequently, cells were selected either for shRNA or CRISPR guide RNA vector positive clones against 5 μg/ml puromycin containing media. A limited dilution method was used to select SH-SY5Y LEO1KO isogenic puromycin-resistant colonies and periodically checked by standard western blotting to measure LEO1 expression. Stable cell lines were maintained in normal culture media with puromycin.

Laser microirradiation and confocal imaging

Recruitment studies were performed on a Nikon Eclipse TE2000-E microscope integrated with an UltraVIEW VoX 3D imaging system (PerkinElmer, Waltham, MA) and a NL100 nitrogen laser (Stanford Research Systems, Sunny Vale, CA) adjusted via MicroPoint ablation technology (Photonics Instruments, St. Charles, IL) to generate a wavelength of 435 nm. Where indicated, cells were grown in a 20 mm glass bottom confocal dish (VWR, USA) and transfected with the indicated plasmid to express the fluorescent-tagged protein. The region of interest in the cells was irradiated with the laser and images were captured at indicated timepoints using indicated settings of exposure time and intensity.

Cell survival assay

Equal numbers of HeLa, and HeLa LEO1KD cells were seeded and allowed to adhere overnight. To determine UVC light sensitivity, cells were irradiated with UVC (254 nm) at 0, 5, 10, 20 and 30 J/m^2, and further incubated unperturbed for 10 days with fresh media. For cisplatin sensitivity, cells were treated for 24 h with 0.4, 0.8, 1.2, 1.6 and 2 μM cisplatin. Post 24 h treatment, cells were washed with PBS, replenished with fresh media, and incubated for 10 days. Menadione sensitivity was determined by treating cells for 1 h with 50, 100, 200, 300 and 400 μM menadione, and then cells were washed with PBS and incubated with fresh media for 10 days. After 10 days, colonies were fixed with methanol and stained with crystal violet. Colonies with >50 cells were scored to determine survival fraction relative to the mock treated controls.

RNA synthesis recovery assay

Equal numbers of CS1AN, CS1AN-CSB, CS1AN-LEO1KD, CS1AN-CSB LEO1KD, SH-SY5Y or SH-SY5Y LEO1KO cells were plated onto 4 well chamber slides (Lab-Tek, Thermo Fisher Scientific). Cells were exposed to 5 or 10 J/m^2 UVC as indicated, and RNA transcription was measured in cells by assessing 5-ethynyl uridine (EU) incorporation into transcribed RNA as per the Click-iT RNA Imaging Kits manual (Thermo Fisher Scientific). Briefly, cells were incubated with 1 mM EU for 1 h and then fixed with 4% (vol/vol) paraformaldehyde solution (sc-281692, Santa Cruz) for 15 min. After permeabilization, cells were incubated with Click-iT® reaction cocktail for 30 min and washed with Click-iT® reaction rinse buffer. Lastly, DNA was stained with Hoechst 33342 by 1:1000 dilution in PBS, and cells were washed twice with PBS before proceeding to imaging.

Immunofluorescence staining of cyclobutane pyrimidine dimers (CPDs)

Equal numbers of SH-SY5Y and SH-SY5Y LEO1KO cells were seeded and allowed to adhere overnight in 4-well chamber slides (Lab-Tek, Thermo Fisher Scientific). Cells were washed once with PBS and irradiated with 10 J/m^2 UVC. Cells were then fixed by 4% formalin in PBS for 10 min followed by permeabilization by 0.5% Triton X-100 for 5 min at room temperature. Further, cellular DNA was denatured by 2 N HCl for 30 min and then washed 5 times with PBS. Cells were blocked by 20% FBS in PBS for 30 min at room temperature. Cells were incubated with anti-CPDs antibody (MBL, TDM-2 D194-1) for 1 h at room temperature. Cells were then washed five times with PBS and further incubated with Alexa Fluor 594-F(ab')2 fragment of anti-mouse IgG (Invitrogen, A-11020) at room temperature for 30 min. After washing cells five times with PBS, they were mounted in DAPI containing mounting medium and images were captured at indicated timepoints using indicated settings of exposure time and intensity.

Statistical analysis

All results are expressed as the mean ± SEM unless specified in figure legend. Statistical analysis was performed using Prism software, and each method of statistical analysis is specified in the relevant figure legend. $P < 0.05$ was considered statistically significant.

RESULTS

Identification of LEO1 as an Interacting Partner of CSB

To identify potential pathways that engage CSB, we previously conducted a Y2H screen using the full-length protein (FL-CSB) as bait (37). This initial screen identified LEO1, as well as three other proteins, including the 5′ to 3′ exonuclease SNM1A, as strong interacting partners of CSB ((37); Supplementary Table S1). Examining the sequence of the LEO1 prey in the first screen revealed Gly370-Ser568 as the region of interaction with FL-CSB (Figure 1A, text in red). In the previous work (not reported at the time), we also found that the 306 C-terminal residues of CSB were sufficient to facilitate the association with LEO1 (Supplementary Figure S1A).

In a separate Y2H screen performed as part of the study here, we employed the C-terminus (Pro1010-Cys1493) of CSB (C-CSB) as bait. Screening over 70 million independent clones of a human placenta library, LEO1 was again identified as a good confidence interactor of CSB, and notably the only gene to appear on both screen lists (Supplementary Tables S1 and S2). Characterizing the two

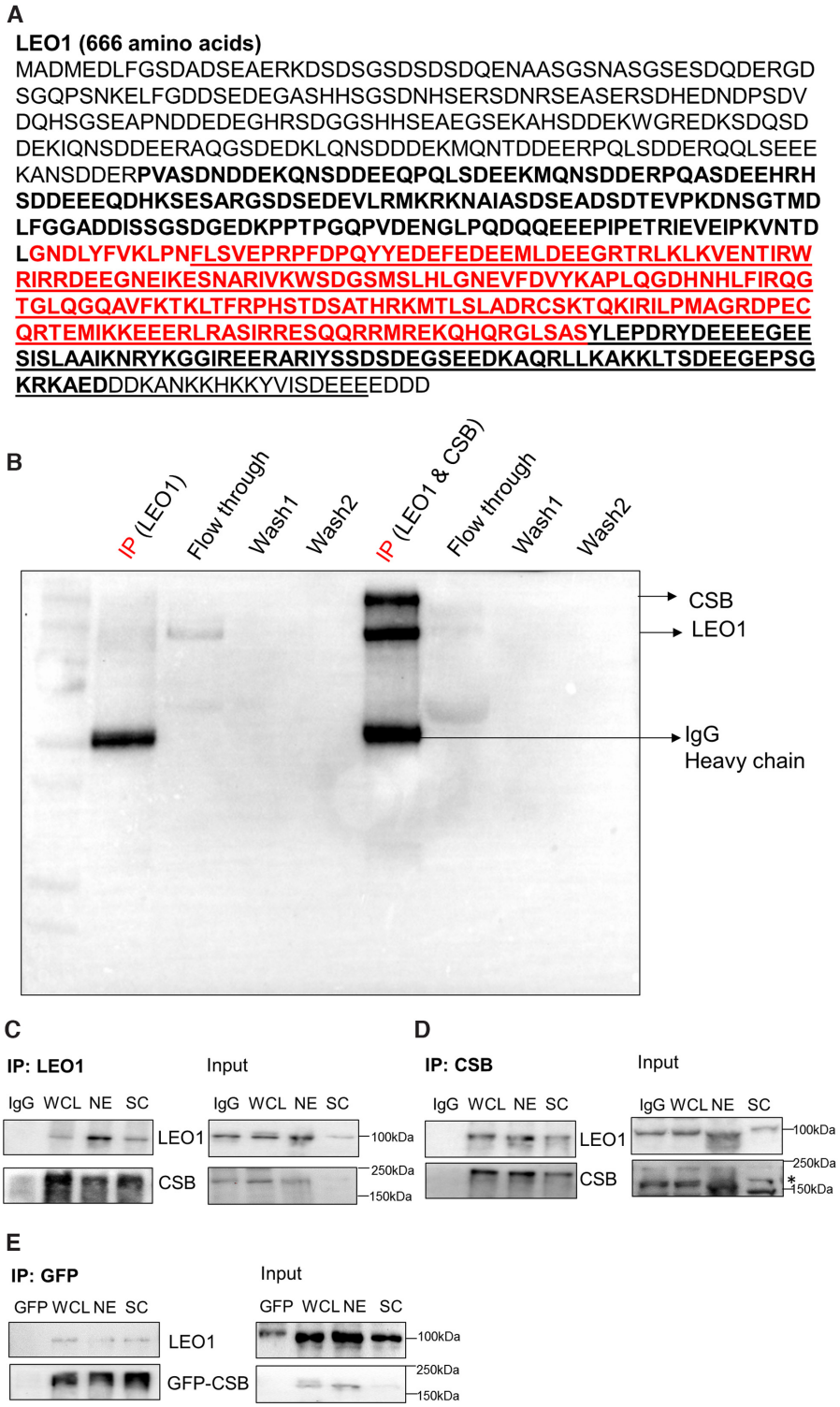

Figure 1. Interaction of CSB with LEO1. (**A**) Region of LEO1 that interacts with CSB. Text in red indicates region of interaction identified in the FL-CSB Y2H screen. Interacting regions identified in the C-CSB Y2H screen are designated by bold and underline. Taken together, the studies reveal Phe381-Ser568 as the common region of interaction with CSB. (**B**) Direct physical interaction of LEO1 and CSB. Recombinant LEO1 (100 ng) was incubated with or without CSB (100 ng), and the interacting complex was captured by anti-CSB antibody in the presence of A/G magnetic beads. Bead-bound material was washed and analyzed by western blot after separation on a Bis-Tris polyacrylamide denaturing gel. (**C–E**) Co-immunoprecipitation (IP) of endogenous CSB and LEO1 from human cell extracts. Whole cell lysate (WCL), nuclear extracts (NE), and soluble chromatin (SC) were prepared from HEK293T cells, and equal protein amounts were incubated with anti-LEO1, CSB, or GFP antibodies as indicated. The IgG lane is the negative control experiment, where WCL was incubated with rabbit or mouse IgG antibody overnight. Antigen-antibody complexes were captured with protein A/G magnetic beads for 1 h, washed, extracted with LDS sampling buffer, and subjected to western blot analysis. * mark represents the expected CSB band.

LEO1 hits uncovered in the C-CSB screen revealed Pro217-Asp644 (bold) and Phe381-Glu662 (underline) to be the interacting regions (Figure 1A). Taken together, our studies find that Phe381-Ser568 of LEO1 interacts with the C-terminus (Pro1010-Cys1493) of CSB (Supplementary Figure S1B).

LEO1 and CSB directly interact and exist in a common complex in human cells

Although the appearance of LEO1 in two independent CSB Y2H screens is a strong indication of a real interaction, validating evidence was sought. First, we checked if purified recombinant forms of CSB and LEO1 (Supplementary Figure S1C) physically interact. Towards that end, we incubated LEO1 with or without CSB, and subsequently immunoprecipitated CSB and examined for the presence of LEO1 by western blot analysis in the different fractions (Figure 1B). Our studies revealed that LEO1 was only captured within the anti-CSB immunoprecipitant when recombinant CSB was present but was otherwise found in the flow-through and presumably (at lower concentrations) in the washes, indicating a direct physical interaction between the two proteins. To explore whether there might be functional consequences of the CSB–LEO1 interaction, we measured the *in vitro* ATPase activity of CSB in the presence of increasing concentrations of LEO1. CSB exhibited the expected DNA-dependent ATPase activity, but there were no observable effects of LEO1 on this CSB function (Supplementary Figure S1D). As LEO1 has no known enzymatic activity, no further *in vitro* analysis was conducted.

Second, we explored whether LEO1 and CSB exist in a common complex within human cells by using co-immunoprecipitation experiments. These efforts revealed that immunoprecipitation of endogenous LEO1 from WCL, NE or SC fractions of HEK293 cells resulted in observable capture of endogenous CSB (Figure 1C). Pull-down of endogenous CSB (HEK293 cells) or GFP-tagged overexpressed CSB (CS1AN cells) from WCL, NE or SC reciprocally co-immunoprecipitated LEO1 (Figure 1D and E, respectively). Since co-immunoprecipitation with the anti-LEO1 antibody was most robust and reliable, we employed this strategy from here on to characterize the LEO1-CSB complex (unless otherwise specified).

Response dynamics of CSB and LEO1 to Genotoxin-induced DNA damage

Given that CSB is involved in the repair of transcription-blocking DNA lesions, such as CPDs and 6–4PPs (3), we examined the dynamics of the LEO1-CSB complex in response to different genotoxic agents, initially using UVC irradiation, looking at WCL and SC prepared from HEK293T cells. We observed an ∼15-fold increase in CSB accumulation with increasing dose of UVC in the SC at 1 h post-exposure, with a more subtle (and variable) change in LEO1 chromatin association (Supplementary Figure S2A); both proteins also appeared to increase in total concentration between 5 and 20 J/m^2 (Figure 2A, input). In addition, the amount of CSB that co-immunoprecipitated with LEO1 increased at higher doses of UVC, up to 30 J/m^2 (Figure 2A, IP:LEO1). Since the LEO1 and CSB response pattern was greatest at 10 J/m^2 UVC (Figure 2A), we used this dose to examine the time-dependent dynamics of these proteins following irradiation. Interestingly, the enhanced association with chromatin of CSB was observed early, at the 1 h time point, tapering off by 3 h, whereas no significant pattern change was seen for LEO1 (Figure 2B, input). Moreover, the highest pulldown of CSB upon immunoprecipitation of LEO1 was recorded at 1 h, with a gradual decrease over 3 h (Supplementary Figure S2B) and remained greater than the no radiation control (Figure 2B, IP:LEO1). Additional fractionation analysis reinforces that CSB gets strongly recruited to chromatin and that the LEO1-CSB interaction is enhanced in response to UVC light-induced DNA damage (Figure 2C).

We next explored the effects of other genotoxins on LEO1 and CSB dynamics. Using cisplatin, which induces various crosslink adducts that can be processed by TC-NER (38), the results resembled those obtained with UVC, with higher recruitment of CSB to chromatin and increased pull down of CSB with anti-LEO1 antibodies in the SC fraction, but little effect on LEO1 overall (Figure 2D, Supplementary Figure S2C). Menadione, an agent that induces oxidative DNA damage, was unique, in that the accumulation of CSB in chromatin following genotoxin exposure was limited, although CSB pull-down with LEO1 was noticeably higher relative to the untreated control (Figure 2E, Supplementary Figure S2C).

Recruitment of CSB and LEO1 to chromatin is transcription-dependent for bulky DNA adducts

Given the involvement of CSB in TC-NER, we asked whether inhibition of transcription would affect recruitment of CSB and/or LEO1 to chromatin following genotoxin exposure. Consistent with prior findings (39,40), pretreatment of cells with DRB, a transcription elongation inhibitor, greatly reduced CSB accumulation (>3-fold) at chromatin in UVC and cisplatin treated HEK293T cells (Figure 3). Moreover, we found that active transcription is also necessary for LEO1 recruitment to damaged chromatin, suggesting a potential role for the protein in a TC-repair response. Notably, recruitment of both CSB and LEO1 to chromatin was independent of active transcription for menadione-induced DNA damage (Figure 3), which consists of mostly oxidative base modifications that are typically less obstructive to DNA and RNA polymerase progression (39). Thus, CSB and LEO1 recruitment to chromatin appears to require stalled RNAPII, a phenomenon that is most prominent at large bulky DNA adducts, such as UV photoproducts and crosslinks (41).

CSB recruitment to chromatin is partly dependent on LEO1

To evaluate the biological significance of the LEO1–CSB interaction, we examined recruitment of CSB to chromatin in wild-type control and LEO1-deficient cells following exposure to a specified genotoxin. Following the establishment of HEK293T and HeLa cell lines where LEO1 expression was knocked-down by targeting shRNA sequences, control and LEO1-deficient cells were exposed to UVC light,

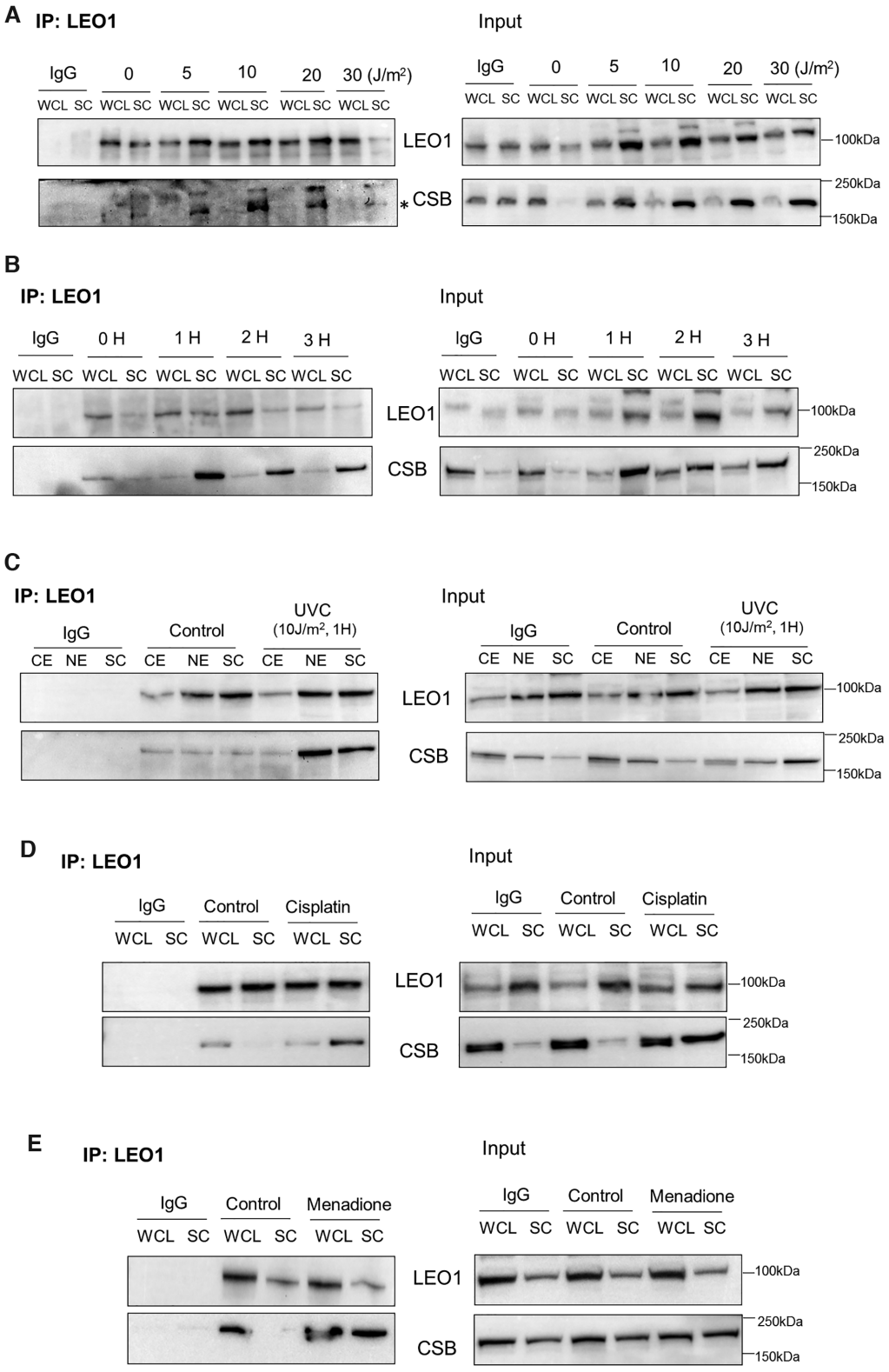

Figure 2. LEO1-CSB coordinately respond to genotoxin induced DNA damage. Co-immunoprecipitation of endogenous CSB and LEO1 in response to genotoxin-induced DNA damage from human HEK293T cell extracts. Whole cell lysate (WCL) and soluble chromatin (SC) extracts were prepared from HEK293T cells, and equal protein amounts were then incubated with anti-LEO1 antibody or control rabbit IgG antibody overnight, and antigen-antibody complexes were subjected to western blot analysis. Dose, time point, or genotoxic agent are indicated. (**A**) WCL and SC extracts were prepared from HEK293T cells 1 h after no (0 J/m^2) or 5, 10, 20 or 30 J/m^2 UVC treatment. *mark represents the expected CSB band. (**B**) LEO1-CSB time course response was evaluated 1, 2 or 3 h after 10 J/m^2 UVC treatment. (**C**) LEO1-CSB complex response in cytosolic (CE), nuclear (NE), and SC fractions 1 h after 10 J/m^2 UVC treatment. WCL and SC extracts were prepared from HEK293T cells either without (control) or with (**D**) 200 μM cisplatin (6 h) or (**E**) 200 μM menadione (1 h) treatment. Anti-LEO1 immunoprecipitated or negative control (IgG) samples are designated.

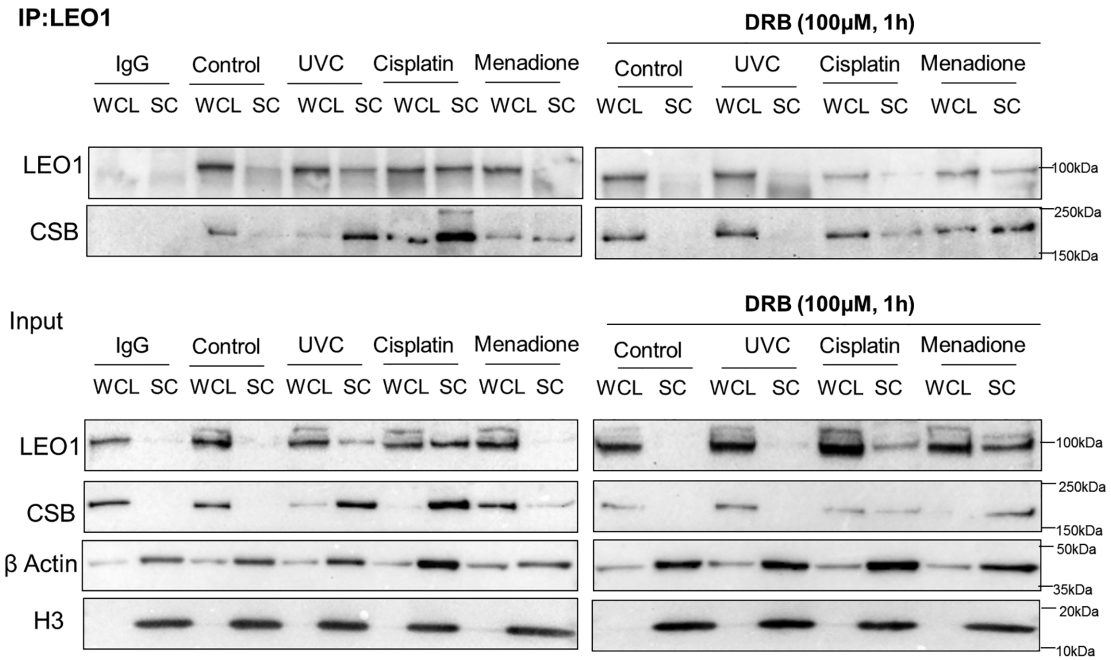

Figure 3. LEO1-CSB interaction is transcription dependent. HEK293T cells were treated with DRB (100 μM) for 1 h and subjected to genotoxin treatment. Whole cell lysate (WCL) and soluble chromatin (SC) extracts were processed as described in Figure 2 legend. Control represents the untreated cells. β-Actin and H3 proteins were employed as fractionation and loading controls.

cisplatin, or menadione, and CSB chromatin association was measured (Figure 4A). As shown, there was significant reduction in CSB recruitment to chromatin in response to UVC and cisplatin induced genomic damage in LEO1-deficient cells as compared to control cells; there was no effect of LEO1 status on CSB accumulation in chromatin following menadione treatment (Figure 4A and B). These data further imply that LEO1 participates in coordination of a transcription-associated repair response through the recruitment of CSB, particularly in cases of well-established transcription blocking adducts.

Coordinated recruitment of LEO1 and CSB to localized DNA damage sites

To examine the recruitment of LEO1 and CSB to localized sites of DNA damage in living cells, we employed a previously established micropoint laser – confocal microscopy set-up (42). Using this approach, we observed that both GFP tagged LEO1 and mcherry tagged CSB recruited to DNA damage sites around the same time (i.e. within 1 min) in HeLa cells (Figure 5A). To examine for possible coordination, we evaluated recruitment of one of the tagged proteins in a cell line deficient in the other protein. Specifically, we observed that mcherry-CSB recruitment was similar in both normal control and LEO1-deficient SH-SY5Y cells (Figure 5B). While these data appear inconsistent with the above chromatin association studies in LEO KD cells described above (Figure 4), the lack of an effect observed here may stem from the high expression of the tagged CSB complementing protein or perhaps the diverse spectrum of DNA damage, which includes oxidative lesions, generated by the laser irradiation (42). Conversely, we found that LEO1 recruitment to localized DNA damage was noticeably reduced (∼2.5-fold; Supplementary Figure S2D) in CSB deficient CS1AN cells relative to CSB corrected cells (Figure 5C). The results collectively suggest that LEO1 and CSB are reciprocally involved in coordinating recruitment at sites of DNA damage and presumably repair.

LEO1 deficiency increases sensitivity to certain genotoxins

Given that LEO1 and CSB communicate at sites of DNA damage, we evaluated the consequence of LEO1 deficiency on genotoxin sensitivity to assess potential functions in DNA repair. Using one of the established LEO1 knockdown cell lines (Figure 6A), we measured comparative cell survival to UVC irradiation, cisplatin and menadione (Figure 6B–D). Relative to shRNA scramble control cells, LEO1-deficient cells were mildly hypersensitive to UVC light (panel B), significantly more hypersensitive to cisplatin (panel C), but not sensitive to menadione (panel D). These results further indicate that LEO1 plays a role in the survival response to DNA damage, particularly to DNA crosslink adducts generated by cisplatin, consistent with a contribution to TC-NER.

LEO1 deficiency impairs RNA synthesis recovery

Since a hallmark of CS cells is the failure to recover RNA synthesis following UVC irradiation due to a defect in TC-NER (43), we examined whether LEO1-deficient cells exhibited a similar phenotype. Employing a previously described method that measures RNA synthesis recovery (RSR) via EU incorporation, we exposed

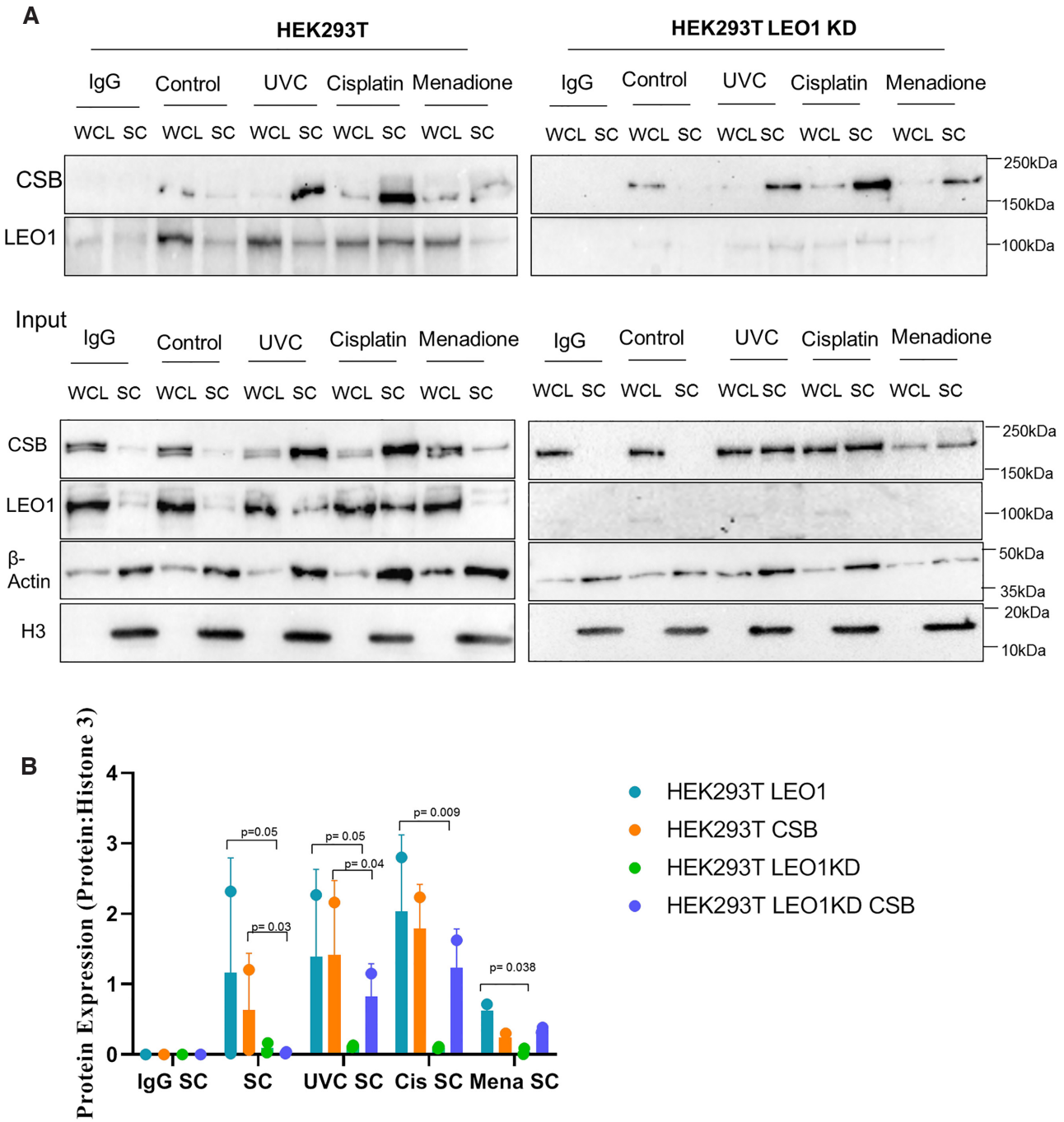

Figure 4. CSB recruitment to chromatin is reduced in LEO1 deficient cells. (**A**) WCL and SC extracts were prepared from HEK293T and LEO1 knockdown (LEO1KD) HEK293T cells treated with UVC (10 J/m^2), cisplatin (200 μM, 6 h) or menadione (200 μM, 1 h), and processed as described in Figure 2 legend. (**B**) Quantitative analysis of protein recruitment to chromatin. Shown is SC association of LEO1 in HEK293T control cells (HEK293T LEO1) and LEO1KD cells (HEK293T LEO1KD LEO1), as well as CSB in the two cell lines. Expression of LEO1 or CSB is plotted relative to histone 3 (H3), a chromatin and loading marker. Mean ± SEM; *t* test was used to determine significant difference on three independent experimental replicates.

CSB-deficient (CS1AN-vector), CSB-corrected (CS1AN-CSB), LEO1-deficient (CS1AN-CSB LEO1 KD), and CSB/LEO1-deficient (CS1AN-vector LEO1 KD) cells to 5 J/m^2 or 10 J/m^2 UVC and quantified EU incorporation at the indicated time points (Supplementary Figures S3 and S4). Whereas our studies revealed the expected impaired RSR profile in CS1AN-vector cells relative to the corrected CS1AN-CSB cell line following 5 J/m^2 or 10 J/m^2 UVC exposure (i.e. ∼25% relative to 99%; Supplementary Figure S3B), LEO1 KD was observed to have little effect on RSR in either the vector or CSB-complemented CS1AN background, suggesting full complementation by residual LEO1 protein (∼95% of normal) or a minor role of LEO1 in the repair response (Supplementary Figure S3B). To ex-

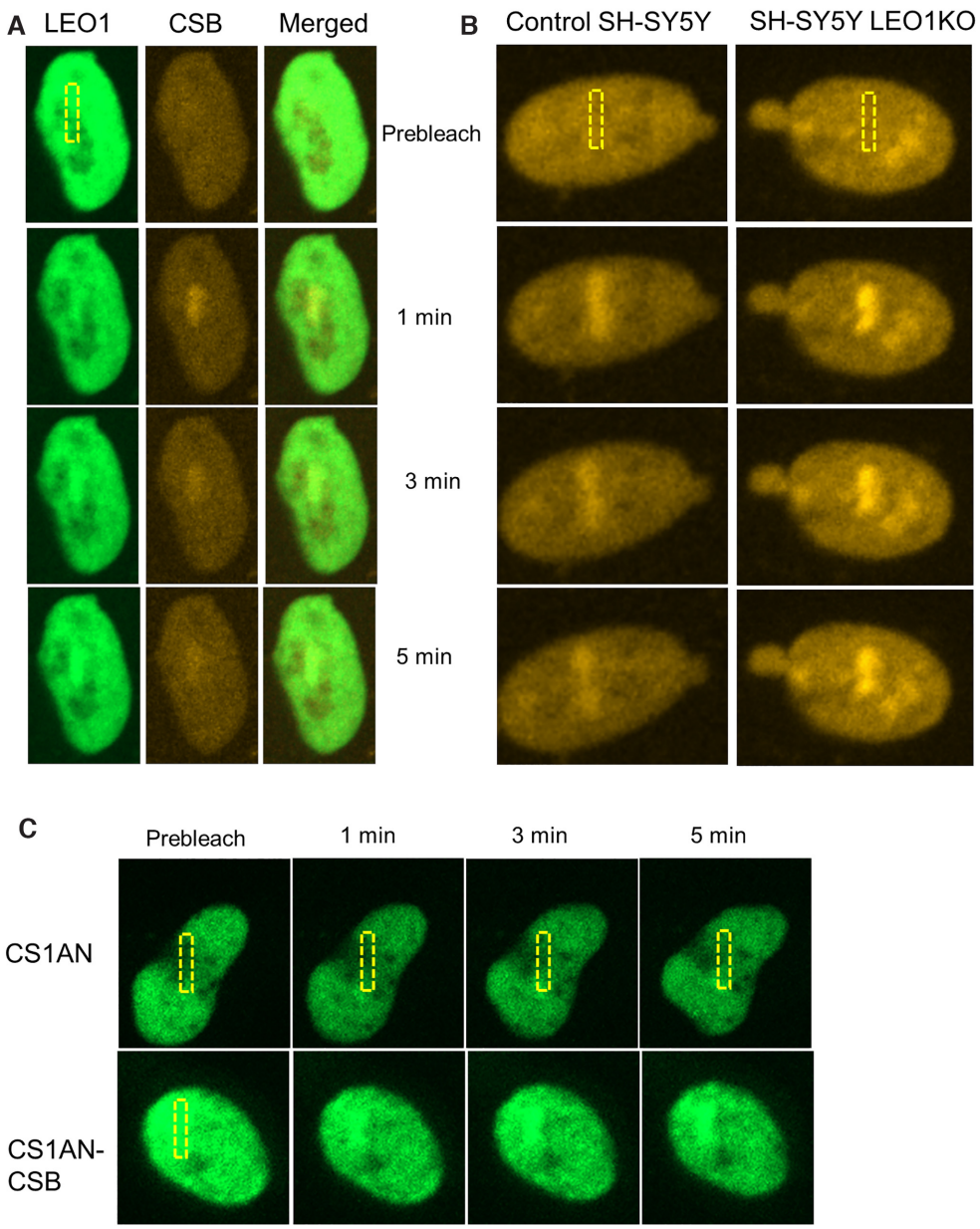

Figure 5. LEO1 and CSB recruitment to site specific DNA damage. (**A**) pLEO1-GFP and pCSB-mcherry were transfected into HeLa cells, and the indicated region (yellow box) was irradiated with a 435 nm laser. Rapid recruitment of LEO1 and CSB is shown and found to overlap (merged). (**B**) pCSB-mcherry was transfected into SH-SY5Y or SH-SY5Y-LEO1KO cells, and CSB recruitment was visualized. (**C**) pLEO1-GFP was transfected into CS1AN and CS1AN-CSB cells, and LEO1 recruitment was found to be reduced in CSB-deficient cells. Yellow boxes indicate areas of laser irradiation. Representative images of unirradiated cells (prebleach) and the LEO1 and/or CSB response at 1, 3 and 5-min post laser irradiation are shown. At least 30 independent cells under each condition were imaged from three independent experiments.

amine these possibilities, we created a LEO1 KO cell line using the CRISPR/Cas9 technology in human SH-SY5Y cells. In these experiments, we observed that LEO1 gene inactivation, which results in no detectable LEO1 protein (Figure 6E), led to a mild, yet reproducible and significant, ∼22% reduction in EU incorporation as compared to UVC irradiated control cells (Figure 6F and G). Our data collectively support a role for LEO1 in helping coordinate a CSB-directed TC-repair process that operates to resolve transcription-blocking lesions, such as UVC photoproducts and cisplatin crosslinks.

LEO1 deficiency results in prolonged CPDs retention

Exposure to UVC light mostly results in the generation of CPDs, which are repaired by the different sub-pathways of NER (3). To examine repair efficiency of CPDs as a function of LEO1 presence, both control SH-SY5Y and SH-SY5Y LEO1 KO cells were exposed to 10 J/m^2 UVC and excision of genomic CPDs was measured using a well-established immunodetection assay (44). As shown in Figure 7, both cell types contained nearly the same number of CPDs immediately after UVC treatment, with CPD levels

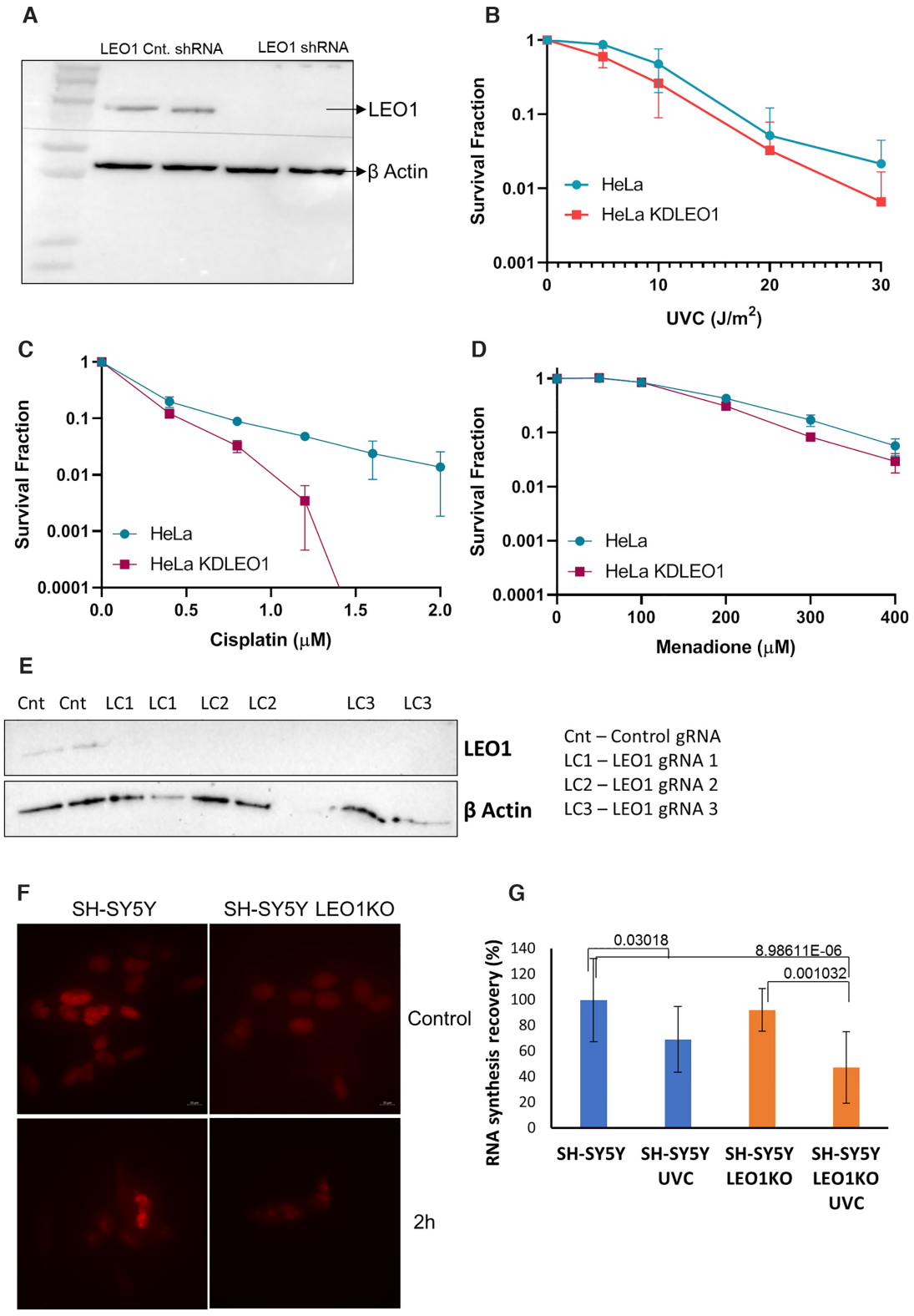

Figure 6. LEO1 deficiency increases sensitivity to UVC and cisplatin treatment. (**A**) Western blot analysis confirming stable knockdown of LEO1 in HeLa cells. Clonogenic survival assay of normal and LEO1-deficient (KDLEO1) HeLa cells against increasing dose of (**B**) UVC, (**C**) cisplatin, or (**D**) menadione. (**E**) Western blot analysis confirming CRISPR/Cas9 inactivation of LEO1 (LEO1KO) in SH-SY5Y cells. Experiments targeting LEO1 were carried out with separate gRNAs, as indicated (see Materials and Methods). (**F**) Representative images of SH-SY5Y and SH-SY5Y LEO1KO cells showing recovery of RNA synthesis (RSR) 2 h after 10 J/m^2 UVC irradiation (shown in red via EU incorporation), after mock or gRNA-mediated knockout of LEO1. All images were captured using similar settings. (**G**) Quantitation of RSR after UVC exposure in SH-SY5Y and SH-SY5Y LEO1KO cells. At least 75 nuclei/group were analyzed in the experiment. Mean ± SD; t test was used to determine significant difference.

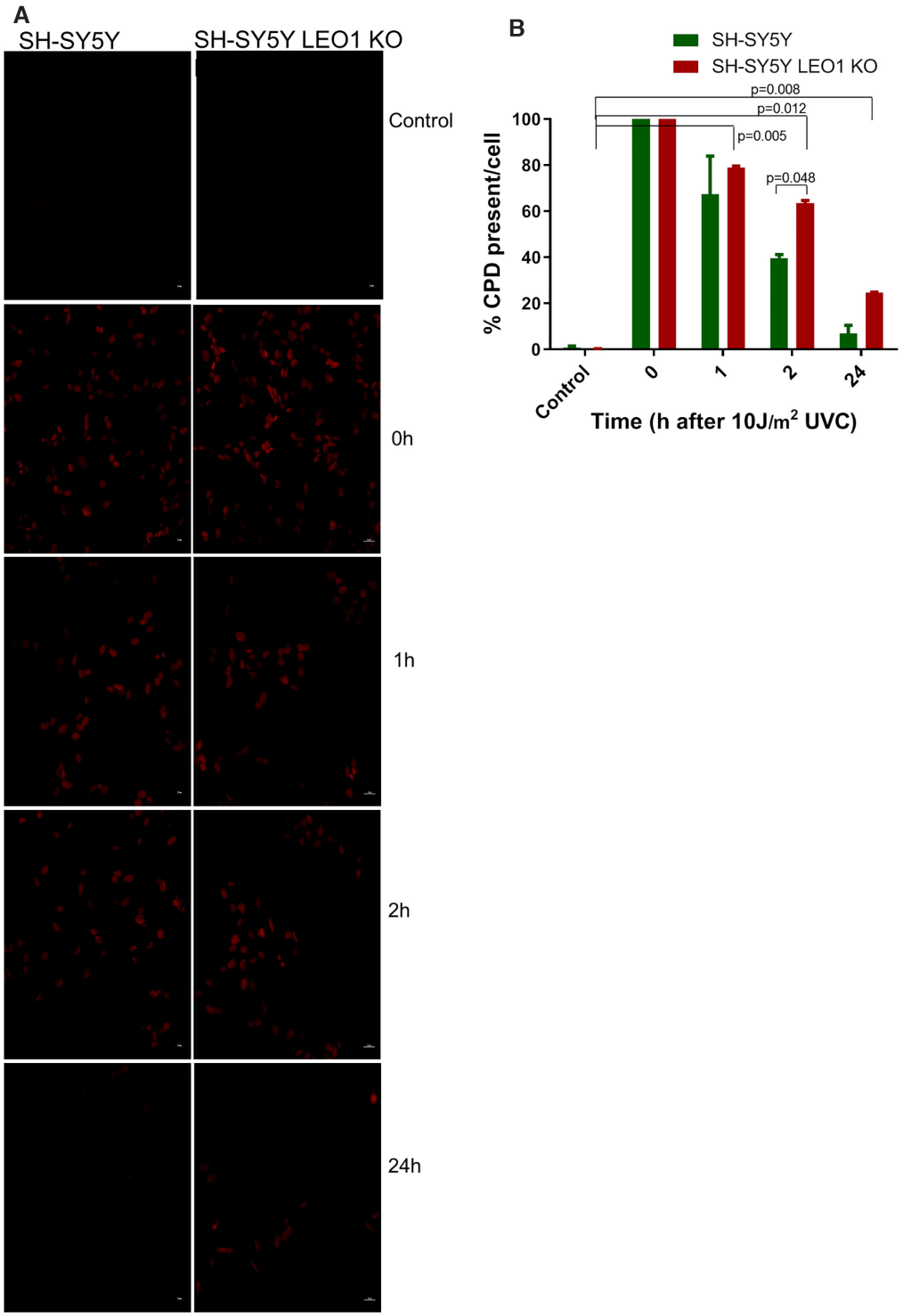

Figure 7. LEO1 deficiency results in prolonged CPDs retention. (**A**) SH-SY5Y and SH-SY5Y LEO1 KO cells were cultured overnight and then irradiated with 10 J/m^2 UVC. Cells were fixed, permeabilized at 0 (immediately after irradiation), 1, 2, and 24 h after UVC exposure. After denaturation of DNA, CPDs were visualized by immunofluorescence with D194-1 antibody and counterstained with DAPI. (**B**) Quantification of CPD retention after UVC exposure in SH-SY5Y and SH-SY5Y LEO1 KO cells. At least 200 nuclei/group were analyzed from two independent experiments for fluorescence intensity. Mean ± SEM; t test was used to determine significance.

gradually decreasing over time. However, the efficiency of removal of CPDs was significantly impaired in SH-SY5Y LEO1 KO cells, with roughly a 4-fold greater number of adducts present at the 24 h time point relative to control cells. These results imply that LEO1 plays a direct role in the repair process for CPDs in response to UV-induced DNA damage.

DISCUSSION

Prior work indicates that CSB plays a vital role in the repair of transcription blocking lesions and in transcription itself (3,37). Specifically, the ATP-dependent chromatin-remodeling factor CSB facilitates efficient removal of bulky DNA damage from the transcribed strand of active genes through the action of well-defined protein participants (45). If unresolved, persistent stalling of RNAPII at such DNA lesions can lead to detrimental cellular outcomes, such as genome-wide transcriptional arrest (46) and apoptosis (47), events that can contribute to the disease etiology of CS. UV induced DNA damage, in particular, can also halt transcription initiation by the transcription repressor ATF3 (27). Hence, it is important for cells to recover and restore transcription after repair to maintain gene expression and cell functionality and viability. Using a Y2H approach (37), we identified LEO1, a PAF1C member, as an interacting partner of CSB, revealing a molecular link between the transcription and repair machinery. The Y2H experiments indicate that the C-terminal portion of CSB interacts with Phe381-Ser568 of LEO1, and our biochemical studies establish evidence for a direct physical interaction between the two proteins. Furthermore, we observed that LEO1 and CSB exist in a common protein complex within human cell extracts, confirming communication between the two proteins *in vivo*.

It has been reported that CSB is involved in the repair of UV induced DNA damage, base-base crosslinks, and certain bulky oxidative damages (4). Our data indicate a coordinated recruitment of LEO1 and CSB to chromatin in response to primarily transcription-blocking DNA lesions, such as generated by UV irradiation and cisplatin. Since both CSB and LEO1 accumulation at transcription-blocking damage was significantly suppressed by DRB treatment, the interaction is seemingly mediated by active RNA transcription, as would be expected for a classic TC-NER response. The reason for the less coordinated response between the two proteins in the case of menadione-induced damage is likely that oxidative DNA lesions are typically not a preferred substrate of TC-NER, but instead of base excision repair (48). Consistently, as previously reported, the global CSB-chromatin association in response to menadione induced oxidative damage is different from UV induced damage, as the latter requires ATP hydrolysis that induces conformational changes in the C-terminal region of CSB (39,40). Thus, our results are consistent with a model whereby the efficient assembly of the TC-repair apparatus and resolution of transcription-blocking DNA adducts is partly reliant on the LEO1-CSB interaction. Consistent with our model (Figure 8), cells deficient in LEO1 exhibit increased sensitivity to certain genotoxins (i.e. UVC light and cisplatin) and display impaired excision of CPDs and defective RSR after UVC light exposure.

Epigenetic alterations, which is a hallmark of aging, have been linked to CS (49). Several chromatin factors like DOT1L (50), the histone chaperones FACT (51), and HIRA (52) have roles in transcriptional restart after DNA damage, and LEO1 is essential for the dynamic regulation of heterochromatin (32). Furthermore, CSB interacts with a number of proteins that regulate various biological functions, including DNA repair, transcription, and RNAPII processing. In particular, CSB interacts with CSA through its CSA-interaction motif (CIM) that is present upstream of the ubiquitin binding domain in its C-terminus (i.e. within the C-CSB fragment) (4). The C-terminus of CSB is also important in regulating UV sensitivity and restoring transcription following UV-induced inhibition (53). We have found that LEO1 also interacts with the C-terminal region of CSB (C-CSB), facilitating the response to transcription blocking lesions such as those introduced by UV light or cisplatin. Based on the data in its entirety, the LEO1-CSB interaction provides a link between the transcription elongation complex, presumably following stalling of a progressing RNA polymerase, to the TC-NER machinery.

Besides the apparent role for LEO1 in helping coordinate CSB at sites of stalled transcription, we also observed that LEO1 deficient cells have reduced CSB recruitment to localized DNA damage. Moreover, LEO1 deficient cells exhibit a prolonged retention of CPDs as compared to normal cells (Figure 7), indicating a key role for the protein in the repair of CPDs. CSB is a conserved helicase ATPase, which is important for the function of the CSB protein in responding to UV-induced DNA damage (54,55). Since LEO1 has no direct effect on the ATPase activity of CSB *in vitro*, we assume that LEO1 acts as scaffold protein, promoting proper orientation and proximity of the various TC-NER factors, including CSB, and improving efficiency of the DNA repair response. Given that TC-NER is in part initiated by CSB, our data indicates that LEO1 is necessary to recruit CSB to sites of DNA damage and improve excision efficiency. While it is well established that CSB is important for initiation of TC-NER, the protein may not be sufficient by itself to resume transcription. Our data suggest that CSB in cooperation with LEO1 alone, or as part of the PAF1C complex, helps assemble the repair machinery at sites of DNA damage.

While in preparation, a very recent report from the Luijsterburg laboratory reported that CSB and the PAF1C operate collaboratively to restore transcription after DNA damage (56). Their study suggests that this interaction is anchored through LEO1 and part of a response to UV induced DNA damage (56). Our research indicates a direct physical contact between LEO1 and CSB, revealing a molecular feature of the interaction that was not present in the prior work. Moreover, our findings suggest that the coordination between LEO1 and CSB goes beyond UV induced DNA damage, and may be important to other bulky adducts, such as crosslinks generated by cisplatin. While the recent publication argued that the PAF1C-CSB interaction was not related to DNA repair, using a more targeted analysis of

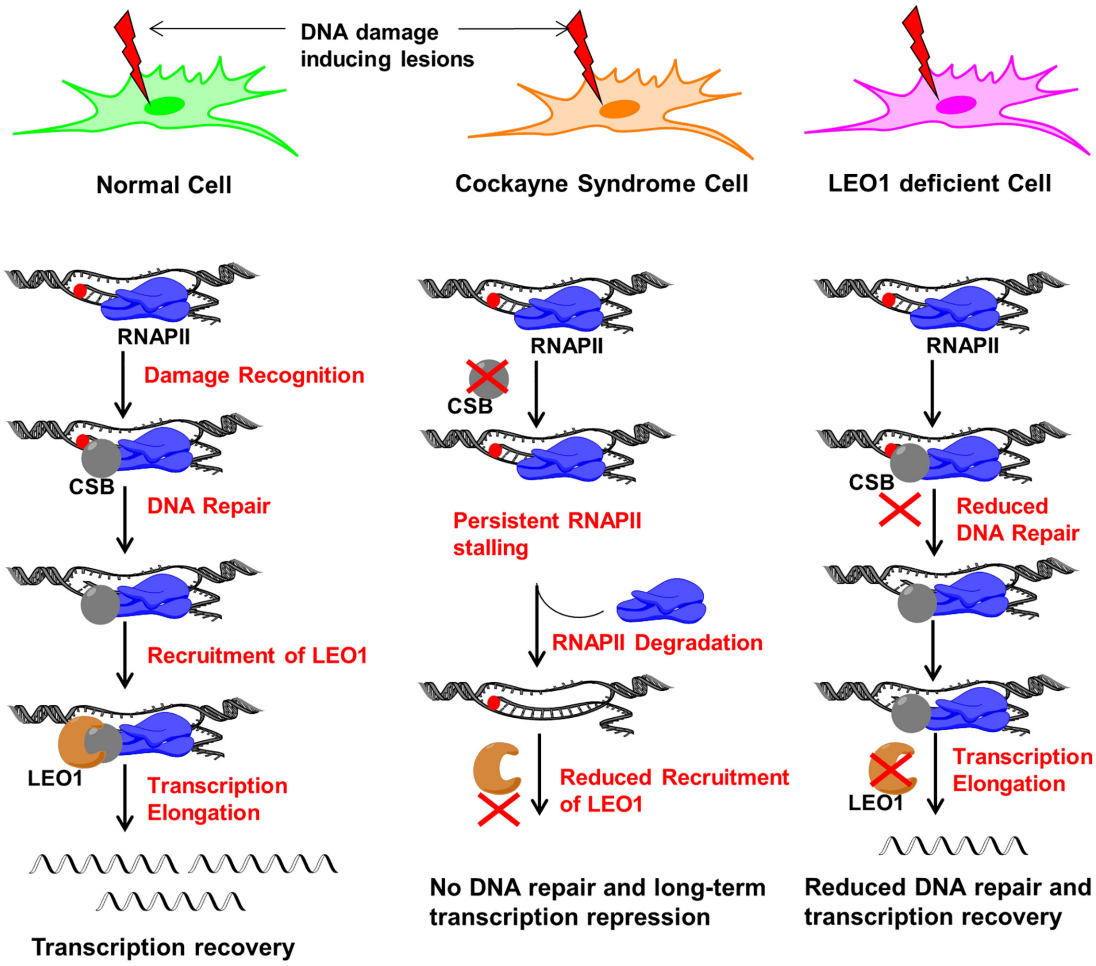

Figure 8. CSB and LEO1 coordinately respond to transcription blocking DNA lesions. In a normal cell (left), DNA blocking damage (red circle) is revealed by stalling of RNA polymerase II (RNAPII). Arrested RNAPII leads to recruitment of the TC-NER factors, like CSB. Following lesion recognition and verification, the damage is excised and repaired by the TC-NER machinery. Thereafter, transcription recovery takes place by recruitment of RNAPII and transcription elongation factors (e.g. LEO1/PAF1C) to restore gene expression. However, in CSB-deficient cells (center), cells are unable to process DNA damage and resolve stalled RNAPII, leading to persistent transcription arrest and dysregulation of downstream proteins, including LEO1/PAF1C, causing failed recovery following genotoxic stress. In LEO1 deficient cells (right), there is reduced recruitment of CSB to chromatin in response to DNA damage, resulting in impaired DNA damage removal and reduced RNA synthesis restoration. Figure was created using artwork of Servier Medical Art and Chemdraw.

CPD removal, we found that LEO1 deficiency results in slower dimer excision, implying that the protein coordination is relevant to both DNA repair and transcription recovery. Thus, our findings here, coupled with recent work (56), have uncovered a reciprocal communication between CSB and LEO1 that functions not only to resolve the stalled RNA polymerase and restart transcription elongation, but to facilitate the repair process.

SUPPLEMENTARY DATA

Supplementary Data are available at NAR Online.

ACKNOWLEDGEMENTS

We thank Drs. Mustafa N Okur and Jong-Hyuk Lee (NIA) for their helpful comments on the article. We thank Alfred May for this support for micro-point laser microscopy.

FUNDING

Intramural Research Program at the NIH, National Institute on Aging. Funding for open access charge: NIH.
Conflict of interest statement. None declared.

REFERENCES

1. Vessoni,A.T., Guerra,C.C.C., Kajitani,G.S., Nascimento,L.L.S. and Garcia,C.C.M. (2020) Cockayne Syndrome: the many challenges and approaches to understand a multifaceted disease. *Genet. Mol. Biol.*, **43**, e20190085.
2. Karikkineth,A.C., Scheibye-Knudsen,M., Fivenson,E., Croteau,D.L. and Bohr,V.A. (2017) Cockayne syndrome: clinical features, model systems and pathways. *Ageing Res. Rev.*, **33**, 3–17.
3. Tiwari,V. and Wilson,D.M. 3rd (2019) DNA damage and associated DNA repair defects in disease and premature aging. *Am. J. Hum. Genet.*, **105**, 237–257.
4. Tiwari,V., Baptiste,B.A., Okur,M.N. and Bohr,V.A. (2021) Current and emerging roles of Cockayne syndrome group B (CSB) protein. *Nucleic Acids Res.*, **49**, 2418–2434.

5. Fischer,E.S., Scrima,A., Böhm,K., Matsumoto,S., Lingaraju,G.M., Faty,M., Yasuda,T., Cavadini,S., Wakasugi,M., Hanaoka,F. *et al.* (2011) The molecular basis of CRL4DDB2/CSA ubiquitin ligase architecture, targeting, and activation. *Cell*, **147**, 1024–1039.
6. Boetefuer,E.L., Lake,R.J. and Fan,H.Y. (2018) Mechanistic insights into the regulation of transcription and transcription-coupled DNA repair by Cockayne syndrome protein B. *Nucleic Acids Res.*, **46**, 7471–7479.
7. Aamann,M.D., Sorensen,M.M., Hvitby,C., Berquist,B.R., Muftuoglu,M., Tian,J., de Souza-Pinto,N.C., Scheibye-Knudsen,M., Wilson,D.M. 3rd, Stevnsner,T. *et al.* (2010) Cockayne syndrome group B protein promotes mitochondrial DNA stability by supporting the DNA repair association with the mitochondrial membrane. *FASEB J.*, **24**, 2334–2346.
8. Lopes,A.F.C., Bozek,K., Herholz,M., Trifunovic,A., Rieckher,M. and Schumacher,B. (2020) A C. elegans model for neurodegeneration in Cockayne syndrome. *Nucleic Acids Res.*, **48**, 10973–10985.
9. Pascucci,B., D'Errico,M., Romagnoli,A., De Nuccio,C., Savino,M., Pietraforte,D., Lanzafame,M., Calcagnile,A.S., Fortini,P., Baccarini,S. *et al.* (2017) Overexpression of parkin rescues the defective mitochondrial phenotype and the increased apoptosis of Cockayne Syndrome A cells. *Oncotarget*, **8**, 102852–102867.
10. Cleaver,J.E., Brennan-Minnella,A.M., Swanson,R.A., Fong,K.W., Chen,J., Chou,K.M., Chen,Y.W., Revet,I. and Bezrookove,V. (2014) Mitochondrial reactive oxygen species are scavenged by Cockayne syndrome B protein in human fibroblasts without nuclear DNA damage. *Proc. Natl. Acad. Sci. U.S.A.*, **111**, 13487–13492.
11. Kamenisch,Y., Fousteri,M., Knoch,J., von Thaler,A.K., Fehrenbacher,B., Kato,H., Becker,T., Dollé,M.E., Kuiper,R., Majora,M. *et al.* (2010) Proteins of nucleotide and base excision repair pathways interact in mitochondria to protect from loss of subcutaneous fat, a hallmark of aging. *J. Exp. Med.*, **207**, 379–390.
12. Hanawalt,P.C. and Spivak,G. (2008) Transcription-coupled DNA repair: two decades of progress and surprises. *Nat. Rev. Mol. Cell Biol.*, **9**, 958–970.
13. van der Weegen,Y., Golan-Berman,H., Mevissen,T.E.T., Apelt,K., González-Prieto,R., Goedhart,J., Heilbrun,E.E., Vertegaal,A.C.O., van den Heuvel,D., Walter,J.C. *et al.* (2020) The cooperative action of CSB, CSA, and UVSSA target TFIIH to DNA damage-stalled RNA polymerase II. *Nat. Commun.*, **11**, 2104.
14. Nakazawa,Y., Hara,Y., Oka,Y., Komine,O., van den Heuvel,D., Guo,C., Daigaku,Y., Isono,M., He,Y., Shimada,M. *et al.* (2020) Ubiquitination of DNA damage-stalled RNAPII promotes transcription-coupled repair. *Cell*, **180**, 1228–1244.
15. Tufegdžić Vidaković,A., Mitter,R., Kelly,G.P., Neumann,M., Harreman,M., Rodríguez-Martínez,M., Herlihy,A., Weems,J.C., Boeing,S., Encheva,V. *et al.* (2020) Regulation of the RNAPII Pool Is Integral to the DNA Damage Response. *Cell*, **180**, 1245–1261.
16. van den Boom,V., Citterio,E., Hoogstraten,D., Zotter,A., Egly,J.M., van Cappellen,W.A., Hoeijmakers,J.H., Houtsmuller,A.B. and Vermeulen,W. (2004) DNA damage stabilizes interaction of CSB with the transcription elongation machinery. *J. Cell Biol.*, **166**, 27–36.
17. Xu,J., Lahiri,I., Wang,W., Wier,A., Cianfrocco,M.A., Chong,J., Hare,A.A., Dervan,P.B., DiMaio,F., Leschziner,A.E. *et al.* (2017) Structural basis for the initiation of eukaryotic transcription-coupled DNA repair. *Nature*, **551**, 653–657.
18. Selvam,K., Ding,B., Sharma,R. and Li,S. (2019) Evidence that moderate eviction of Spt5 and promotion of error-free transcriptional bypass by Rad26 facilitates transcription coupled nucleotide excision repair. *J. Mol. Biol.*, **431**, 1322–1338.
19. Charlet-Berguerand,N., Feuerhahn,S., Kong,S.E., Ziserman,H., Conaway,J.W., Conaway,R. and Egly,J.M. (2006) RNA polymerase II bypass of oxidative DNA damage is regulated by transcription elongation factors. *EMBO J.*, **25**, 5481–5491.
20. Tu,Y., Bates,S. and Pfeifer,G.P. (1998) The transcription-repair coupling factor CSA is required for efficient repair only during the elongation stages of RNA polymerase II transcription. *Mutat. Res.*, **400**, 143–151.
21. Newman,J.C., Bailey,A.D. and Weiner,A.M. (2006) Cockayne syndrome group B protein (CSB) plays a general role in chromatin maintenance and remodeling. *Proc. Natl. Acad. Sci. U.S.A.*, **103**, 9613–9618.
22. Lake,R.J., Boetefuer,E.L., Tsai,P.F., Jeong,J., Choi,I., Won,K.J. and Fan,H.Y. (2014) The sequence-specific transcription factor c-Jun targets Cockayne syndrome protein B to regulate transcription and chromatin structure. *PLos Genet.*, **10**, e1004284.
23. Kyng,K.J., May,A., Brosh,R.M., Cheng,W.H., Chen,C., Becker,K.G. and Bohr,V.A. (2003) The transcriptional response after oxidative stress is defective in Cockayne syndrome group B cells. *Oncogene*, **22**, 1135–1149.
24. Lee,B.K. and Iyer,V.R. (2012) Genome-wide studies of CCCTC-binding factor (CTCF) and cohesin provide insight into chromatin structure and regulation. *J. Biol. Chem.*, **287**, 30906–30913.
25. Ong,C.T. and Corces,V.G. (2014) CTCF: an architectural protein bridging genome topology and function. *Nat. Rev. Genet.*, **15**, 234–246.
26. Wang,Y., Chakravarty,P., Ranes,M., Kelly,G., Brooks,P.J., Neilan,E., Stewart,A., Schiavo,G. and Svejstrup,J.Q. (2014) Dysregulation of gene expression as a cause of Cockayne syndrome neurological disease. *Proc. Natl. Acad. Sci. U.S.A.*, **111**, 14454–14459.
27. Epanchintsev,A., Costanzo,F., Rauschendorf,M.A., Caputo,M., Ye,T., Donnio,L.M., Proietti-de-Santis,L., Coin,F., Laugel,V. and Egly,J.M. (2017) Cockayne's syndrome A and B proteins regulate transcription arrest after genotoxic stress by promoting ATF3 degradation. *Mol. Cell*, **68**, 1054–1066.
28. Epanchintsev,A., Rauschendorf,M.A., Costanzo,F., Calmels,N., Obringer,C., Sarasin,A., Coin,F., Laugel,V. and Egly,J.M. (2020) Defective transcription of ATF3 responsive genes, a marker for Cockayne Syndrome. *Sci. Rep.*, **10**, 1105.
29. Latini,P., Frontini,M., Caputo,M., Gregan,J., Cipak,L., Filippi,S., Kumar,V., Vélez-Cruz,R., Stefanini,M. and Proietti-De-Santis,L. (2011) CSA and CSB proteins interact with p53 and regulate its Mdm2-dependent ubiquitination. *Cell Cycle*, **10**, 3719–3730.
30. Groisman,R., Polanowska,J., Kuraoka,I., Sawada,J., Saijo,M., Drapkin,R., Kisselev,A.F., Tanaka,K. and Nakatani,Y. (2003) The ubiquitin ligase activity in the DDB2 and CSA complexes is differentially regulated by the COP9 signalosome in response to DNA damage. *Cell*, **113**, 357–367.
31. Groisman,R., Kuraoka,I., Chevallier,O., Gaye,N., Magnaldo,T., Tanaka,K., Kisselev,A.F., Harel-Bellan,A. and Nakatani,Y. (2006) CSA-dependent degradation of CSB by the ubiquitin-proteasome pathway establishes a link between complementation factors of the Cockayne syndrome. *Genes Dev.*, **20**, 1429–1434.
32. Oya,E., Durand-Dubief,M., Cohen,A., Maksimov,V., Schurra,C., Nakayama,J.I., Weisman,R., Arcangioli,B. and Ekwall,K. (2019) Leo1 is essential for the dynamic regulation of heterochromatin and gene expression during cellular quiescence. *Epigenetics Chromatin*, **12**, 45.
33. Gaillard,H., Tous,C., Botet,J., González-Aguilera,C., Quintero,M.J., Viladevall,L., García-Rubio,M.L., Rodríguez-Gil,A., Marín,A., Ariño,J. *et al.* (2009) Genome-wide analysis of factors affecting transcription elongation and DNA repair: a new role for PAF and Ccr4-not in transcription-coupled repair. *PLos Genet.*, **5**, e1000364.
34. Tatum,D., Li,W., Placer,M. and Li,S. (2011) Diverse roles of RNA polymerase II-associated factor 1 complex in different subpathways of nucleotide excision repair. *J. Biol. Chem.*, **286**, 30304–30313.
35. Berquist,B.R. and Wilson,D.M. 3rd (2009) Nucleic acid binding activity of human Cockayne syndrome B protein and identification of Ca(2+) as a novel metal cofactor. *J. Mol. Biol.*, **391**, 820–832.
36. Scheibye-Knudsen,M., Ramamoorthy,M., Sykora,P., Maynard,S., Lin,P.C., Minor,R.K., Wilson,D.M., Cooper,M., Spencer,R., de Cabo,R. *et al.* (2012) Cockayne syndrome group B protein prevents the accumulation of damaged mitochondria by promoting mitochondrial autophagy. *J. Exp. Med.*, **209**, 855–869.
37. Iyama,T., Lee,S.Y., Berquist,B.R., Gileadi,O., Bohr,V.A., Seidman,M.M., McHugh,P.J. and Wilson,D.M. 3rd (2015) CSB interacts with SNM1A and promotes DNA interstrand crosslink processing. *Nucleic. Acids. Res.*, **43**, 247–258.
38. Furuta,T., Ueda,T., Aune,G., Sarasin,A., Kraemer,K.H. and Pommier,Y. (2002) Transcription-coupled nucleotide excision repair as a determinant of cisplatin sensitivity of human cells. *Cancer Res.*, **62**, 4899–4902.
39. Boetefuer,E.L., Lake,R.J., Dreval,K. and Fan,H.Y. (2018) Poly(ADP-ribose) polymerase 1 (PARP1) promotes oxidative stress-induced association of Cockayne syndrome group B protein with chromatin. *J. Biol. Chem.*, **293**, 17863–17874.
40. Lake,R.J., Geyko,A., Hemashettar,G., Zhao,Y. and Fan,H.Y. (2010) UV-induced association of the CSB remodeling protein with

chromatin requires ATP-dependent relief of N-terminal autorepression. *Mol. Cell*, **37**, 235–246.
41. Lans,H., Hoeijmakers,J.H.J., Vermeulen,W. and Marteijn,J.A. (2019) The DNA damage response to transcription stress. *Nat. Rev. Mol. Cell Biol.*, **20**, 766–784.
42. Iyama,T. and Wilson,D.M. 3rd (2016) Elements that regulate the DNA damage response of proteins defective in Cockayne Syndrome. *J. Mol. Biol.*, **428**, 62–78.
43. Mayne,L.V. and Lehmann,A.R. (1982) Failure of RNA synthesis to recover after UV irradiation: an early defect in cells from individuals with Cockayne's syndrome and xeroderma pigmentosum. *Cancer Res.*, **42**, 1473–1478.
44. Matsumoto,M., Yaginuma,K., Igarashi,A., Imura,M., Hasegawa,M., Iwabuchi,K., Date,T., Mori,T., Ishizaki,K., Yamashita,K. *et al.* (2007) Perturbed gap-filling synthesis in nucleotide excision repair causes histone H2AX phosphorylation in human quiescent cells. *J. Cell Sci.*, **120**, 1104–1112.
45. Citterio,E., Van Den Boom,V., Schnitzler,G., Kanaar,R., Bonte,E., Kingston,R.E., Hoeijmakers,J.H. and Vermeulen,W. (2000) ATP-dependent chromatin remodeling by the Cockayne syndrome B DNA repair-transcription-coupling factor. *Mol. Cell. Biol.*, **20**, 7643–7653.
46. Brueckner,F., Hennecke,U., Carell,T. and Cramer,P. (2007) CPD damage recognition by transcribing RNA polymerase II. *Science*, **315**, 859–862.
47. Ljungman,M. and Zhang,F. (1996) Blockage of RNA polymerase as a possible trigger for u.v. light-induced apoptosis. *Oncogene*, **13**, 823–831.
48. Kitsera,N., Stathis,D., Luhnsdorf,B., Muller,H., Carell,T., Epe,B. and Khobta,A. (2011) 8-Oxo-7,8-dihydroguanine in DNA does not constitute a barrier to transcription, but is converted into transcription-blocking damage by OGG1. *Nucleic Acids Res.*, **39**, 5926–5934.
49. Lee,J.H., Demarest,T.G., Babbar,M., Kim,E.W., Okur,M.N., De,S., Croteau,D.L. and Bohr,V.A. (2019) Cockayne syndrome group B deficiency reduces H3K9me3 chromatin remodeler SETDB1 and exacerbates cellular aging. *Nucleic. Acids. Res.*, **47**, 8548–8562.
50. Oksenych,V., Zhovmer,A., Ziani,S., Mari,P.O., Eberova,J., Nardo,T., Stefanini,M., Giglia-Mari,G., Egly,J.M. and Coin,F. (2013) Histone methyltransferase DOT1L drives recovery of gene expression after a genotoxic attack. *PLoS Genet.*, **9**, e1003611.
51. Dinant,C., Ampatziadis-Michailidis,G., Lans,H., Tresini,M., Lagarou,A., Grosbart,M., Theil,A.F., van Cappellen,W.A., Kimura,H., Bartek,J. *et al.* (2013) Enhanced chromatin dynamics by FACT promotes transcriptional restart after UV-induced DNA damage. *Mol. Cell*, **51**, 469–479.
52. Adam,S., Polo,S.E. and Almouzni,G. (2013) Transcription recovery after DNA damage requires chromatin priming by the H3.3 histone chaperone HIRA. *Cell*, **155**, 94–106.
53. Anindya,R., Mari,P.O., Kristensen,U., Kool,H., Giglia-Mari,G., Mullenders,L.H., Fousteri,M., Vermeulen,W., Egly,J.M. and Svejstrup,J.Q. (2010) A ubiquitin-binding domain in Cockayne syndrome B required for transcription-coupled nucleotide excision repair. *Mol. Cell*, **38**, 637–648.
54. Selzer,R.R., Nyaga,S., Tuo,J., May,A., Muftuoglu,M., Christiansen,M., Citterio,E., Brosh,R.M. Jr and Bohr,V.A. (2002) Differential requirement for the ATPase domain of the Cockayne syndrome group B gene in the processing of UV-induced DNA damage and 8-oxoguanine lesions in human cells. *Nucleic Acids Res.*, **30**, 782–793.
55. Brosh,R.M. Jr, Balajee,A.S., Selzer,R.R., Sunesen,M., Proietti De Santis,L. and Bohr,V.A. (1999) The ATPase domain but not the acidic region of Cockayne syndrome group B gene product is essential for DNA repair. *Mol. Biol. Cell*, **10**, 3583–3594.
56. van den Heuvel,D., Spruijt,C.G., González-Prieto,R., Kragten,A., Paulsen,M.T., Zhou,D., Wu,H., Apelt,K., van der Weegen,Y., Yang,K. *et al.* (2021) A CSB-PAF1C axis restores processive transcription elongation after DNA damage repair. *Nat. Commun.*, **12**, 1342.